*J Forensic Sci,* March 2009, Vol. 54, No. 2
doi: 10.1111/j.1556-4029.2008.00977.x
Available online at: www.blackwell-synergy.com

*Nicholas V. Passalacqua,*[1] *M.S.*

# Forensic Age-at-Death Estimation from the Human Sacrum*

**ABSTRACT:** A new method is described here that incorporates seven developmental and degenerative changes for estimating chronological age from morphological features of the human sacrum. The construction of this method involved multiple stages of trait identification, character-state definition and age correlation, rank-order phase development, and percent-correct sample testing with phase and sample aggregation, all of which resulted in a six-phase component system for application on modern individuals. This phase system was first developed on European American male and female samples from the Hamann-Todd collection; then tested on African American male and female Hamann-Todd samples as well as European American male and females from the WM Bass collection to examine possible sex and/or ancestry differences. Variation in age estimates due to sex and ancestry was negligible; thus, the multiple samples were all pooled creating a robust method with a large sample size. Overall age ranges increase in width at two standard deviations as is expected from degenerative age-related processes but retain utility in forensic situations.

**KEYWORDS:** forensic science, forensic anthropology, age-at-death estimation, sacrum, auricular surface, sacro-iliac joint

Accurate age-at-death estimates are important components of bioarchaeology and other population-focused studies in that they provide key baselines for assessing the applicability and reliability of estimates of other biological parameters such as sex and stature. In addition, they are essential for inferring derived demographic parameters such as growth rates, fertility schedules, and life expectancies (1,2 and references therein). In forensic anthropological contexts, accurate age-at-death estimates are crucial in efforts to positively identify partially or wholly decomposed individuals by narrowing down the missing persons list of potential victims.

Unlike sex or stature, the reliability of age markers is strongly related to the age class of the individual under study. While *developmental* processes such as epiphyseal fusion or dental eruption patterns typically provide rather accurate chronological age estimates for juvenile or immature individuals, *degenerative* processes such as the later metamorphic stages observed in symphyseal surfaces are more useful in assessing the age of older individuals. Furthermore, developmental and degenerative processes affect different anatomical structures at different stages in the life history of the individual. As such, their imprint will be more or less regularly patterned and recognizable depending on the life stage and structure being observed. Therefore, the development of new aging methods based on alternative anatomical areas is an important endeavor as it should improve the estimates for age at least in the age class, where the new elements may better reflect the chronological metamorphoses.

Reliable aging techniques are available for many different anatomical regions of the human body, including: cranial sutures (3,4), epiphyseal-diaphyseal fusion (5,6), pubic symphysis (7), auricular surface of the ilium (8,9), sternal rib ends (10), and dentition (11). However, at times one or more of these diagnostic areas may not be available for analysis in archaeological or paleontological materials due to destructive taphonomic processes or commingling factors; thus, it is important to develop reliable aging techniques for a variety of different skeletal regions.

Forensic applications require an accuracy that is lacking in most bioarchaeological and seriation methodologies (see 12 for discussion on accuracy and precision). Bioarchaeological methods are less concerned about the possibility of victim exclusion due to inaccurate age estimation and focus instead on seriating the entire burial sample to study populational trends. In a forensic context, the focus is on the *individual*, providing an assessment of age that does not exclude the individual from the missing persons list. These fundamental differences in goals result in differing levels of acceptance of potential estimate error. While bioarcheological techniques are precise, these techniques are usually inaccurate. An individual aged with these techniques will potentially fall outside of the smaller confidence intervals (1 standard deviation) 30% of the time. Forensic techniques require different results. They must be accurate, though this entails providing imprecise age estimates with ranges which will correctly classify an individual at least 95% of the time. Furthermore, the reporting of error statistics in forensic science applications is necessary concerning legal admissibility as per the Daubert Guidelines (13); however, in bioarcheological scenarios, there are no such constraints.

The development of new techniques must consider these differing perspectives. In general, if the correct sampling and analytical procedures are applied, a new aging technique will improve existing methods only when it is capable of providing narrower confidence intervals for the obtained age estimates. All methods should provide narrow (1 standard deviation—68% probability) and wide (2 standard deviations—95% probability) ranges. This would allow for easier comparison to other methods which use the same measure of prediction and, in effect, standardize methodologies (14).

The study of ''new'' skeletal regions for age-related changes, such as the sacrum, can help to narrow confidence intervals in two different ways that are not mutually exclusive: (i) it may reveal new processes strongly correlated with age that are not observable in other structures and (ii) traits related to processes affecting other diagnostic areas may be easier to observe in the new structure, reducing uncertainty related to intra- and interobserver error rates.

[1]Department of Anthropology, Michigan State University, East Lansing, MI 48824.

*Presented in part at the 59th Annual Meeting of the American Academy of Forensic Sciences, San Antonio, TX, February19–24, 2007.

Received 20 Jan. 2008; and in revised form 25 Mar. 2008; accepted 18 Oct. 2008.

The sacrum is particularly useful for age estimation because a number of clearly defined developmental changes such as fusion of the first sacral body vertebral epiphysis, occur well into the adult life stage of the individual, a time when most other developmental changes within the skeleton are complete. The sacrum is a bone with 21 primary ossification centers and four areas of articulation to other age-diagnostic surfaces (two auricular surfaces, one vertebral plate, and the occasionally fusing coccyx). The sacrum itself exhibits age-related changes in early, middle, and late childhood (fusion of the bodies), through early to middle adulthood (auricular surface changes), and even later stages of adulthood (osteophytic activity). Despite this obvious utility, the sacrum has been almost completely ignored for adolescent and adult age-at-death estimation (5,8).

The auricular surface of the ilium has received much recent interest as an effective skeletal marker of age (8,9,15–17). However, methods for assessing morphological changes in the auricular surface of the ilium in association with age are often perceived as difficult to apply. Furthermore, because the sacral auricular surface does not undergo the same morphological changes as the ilium auricular surface, there can be no direct comparison. The sacral auricular surface lacks the same billows and striations of the corresponding ilium auricular surface likely due to much thicker hyaline cartilage and much thinner cortical bone than the paired ilium of the sacro-iliac joint (18). By studying the sacrum, the shared characteristics between the sacral and ilium auricular surfaces might be used to gain insight into the origin of these morphological changes and how these metamorphoses progress in the structure of the bone.

Previous research dealing with age estimation from the sacrum is limited. McKern and Stewart (5), studied sacral body fusion patterns and concluded that while definable morphological changes occur on the lateral auricular joints, it was not possible to use them for age-at-death estimation. The next major discussion of sacral aging is found dispersed in the ilium auricular surface aging method described by Lovejoy et al. (8). They also stated that the sacrum cannot be used for accurate age-at-death estimation, though they mentioned that a plate-like epiphysis fuses to the lateral portion of the sacrum in young adulthood (19). Research has been conducted on changes in the cartilaginous component of the sacral auricular surface (18,20), but these changes cannot be easily correlated to bony indicators. Scheuer and Black (6) provided an in-depth discussion of the sacral epiphyses.

The fusion and absorption of vertebral annular epiphyses to the body of thoracic vertebral elements have been studied and shown to be a reliable predictor of age (21–24). However, the trait has not been studied in the lower lumbro-sacral vertebrae.

The method proposed herein will incorporate components of a number of previously described methodologies to different regions of the sacrum, resulting in an assemblage of criteria for estimating age in one osteological structure.

The objectives of the current study were fourfold: (i) identify and determine whether morphological changes observed in the auricular surface of the sacrum and associated structures (seemingly mirroring the age-related processes observed in the conjoining structure of the ilium) can be statistically correlated with chronological age; (ii) prioritize traits in terms of their utility to predict age; (iii) develop confidence intervals (1 and 2 standard deviations) for each age marker; and (iv) test the method on an independent sample.

The approach to age-at-death estimation taken in this research project is relatively unique. The criteria for evaluating morphologic traits will primarily be on a presence/absence basis and numerically expressed via binomial variables. This approach differs from most age estimation techniques such as the Suchey and Katz pubic symphyseal study (7), and Lovejoy et al.'s work on the auricular surface (8), which focus on qualitative skeletal keys that can be difficult to assess. The newly proposed method analyzes each trait individually and assesses what the age might be as a whole avoiding the more general qualitative model.

## Materials

In the construction of the new aging method, a sample of 384 paired ilia and sacra, ranging in age from 10 to 96 years were chosen from the Hamann-Todd collection and 249 specimens from the WM Bass collection housed at the University of Tennessee, Knoxville. The general composition of each of the subsamples is presented in Fig. 1.

The Hamann-Todd collection at the Cleveland Museum of Natural History (Cleveland, Ohio), consists of roughly 3100 modern human skeletons of both males and females of all ages and mainly of African and European ancestry. The collection was amassed between the years of 1839 and 1938 by both Carl August Hamann and T. Wingate Todd. Most of these skeletal elements are derived from positively identified individuals of known age, but some of the specimens are derived from individuals where age was determined through soft tissue markers (see 25 for further discussion). Efforts were made to avoid pathological specimens and individuals under 10 years old, as these individuals can be aged more accurately using other methodologies. In an attempt to create a balanced sample, 10 individuals were originally sampled for each age decade, pooling those individuals 10–30 years of age and individuals over the age of 70 (26). After some preliminary investigation, additional data were collected from the Hamann-Todd collection to give a more rounded age distribution at age stages, where significant changes between phases were noted.

Following development of phases and marker morphologies on the Hamann-Todd collection (described below), the sample of 249 individuals from a modern forensic population was used to test the efficacy of the new aging technique. These independent test samples were collected using similar criteria as those for the reference Hamann-Todd samples.

## Methods

### *Development of Methodological and Statistical Descriptions*

The construction of an age-at-death method involves a number of complex decisions and statistical confirmations. The initial step is to develop general descriptions of how the sacrum changes over time, these morphologies are then defined and quantified as character states. Data from the Hamann-Todd European American male and female samples were chosen for the preliminary analyses as their reference datasets were the largest and most balanced of all the subsamples (see Fig. 1). To begin, the Spearman correlation of each of the traits and their associated character states against documented age were evaluated. Next, a means of combining the independent traits must be constructed to develop a method using the entire sacral morphological gestalt. At this step, Spearman correlations were employed to generate rank order statistics to determine trait change sequencing. From this information, a *sequential coding component system* was developed. Character state scores for each of the eight traits were arranged to produce a dummy variable expressed as a seven-digit code (only seven traits are used in the final age estimate as the trait of coccygeal fusion was not found to be correlated with age). These statistics were selected to obtain a coding system in which a higher score in the generated seven-digit code corresponded more frequently to an older individual. Each unique seven-digit component code was translated into a verbal

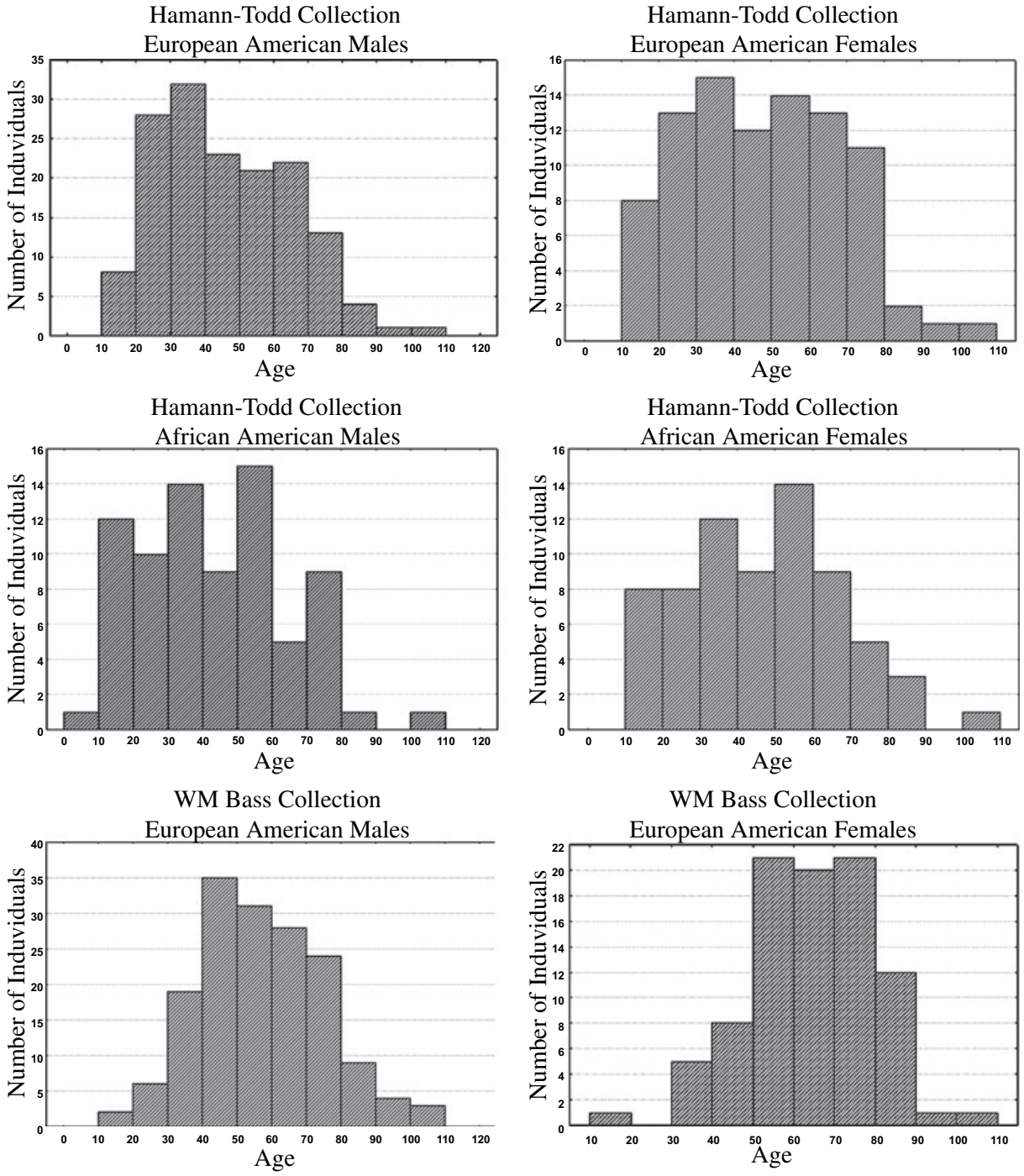


FIG. 1—*Subsample distributions by ancestry and sex.*

description of the combination of morphological traits (morphological stage) and was associated with the appropriate phase and statistically validated chronological confidence interval (presented in standard deviations; 68% and 95% probabilities).

*T*-tests were used to check for discrepancies between phases and differences between left and right side scoring. Finally, each of the subsamples was tested against the Hamann-Todd European American sample to elucidate any ancestry or sex specific biases. To evaluate the performance of the Hamann-Todd European American male and female methods on the other samples, percent correct and inaccuracy were calculated. *Percent correct* is the percentage of individuals correctly classified to a phase based on the confidence interval (here presented in standard deviations). A misclassification of an individual occurs when the individual falls outside of the age range for the phase. This results in a misrepresentation of the age-at-death prediction. *Inaccuracy* rates are calculated by averaging the absolute distance of the phase mean age to the actual age (27).

### Morphologic Traits Analyzed and Character State Definitions

The following eight traits and associated character states were noted for every sacrum in the Hamann-Todd sample and incorporated into the new methodology. Each morphological character was originally scored according to multiple trait variants (specifically three character states), similar to those previously employed in age estimation from the ilium (15).

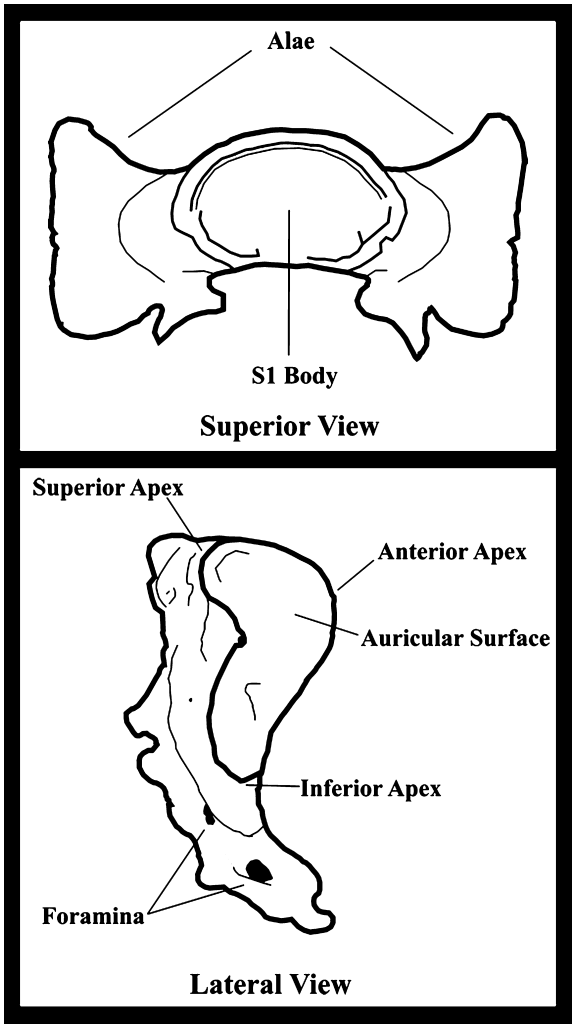


FIG. 2—*Different views of the anatomically dynamic regions of the sacrum in reference to age.*

### *Terminology*

Descriptive terms utilized are similar to, and maintain the meaning of, those used in previous research with the exception of *apex*, which here refers to the rim of bone surrounding the auricular surface (Fig. 2).

### *Sacral Vertebral Body (S1/S2 and S2/S3) Fusion*

Sacral vertebral body fusion is the developmental fusion of the sacral vertebral elements (sacrabrae) to adjacent vertebral bodies to form the single sacral bone. As illustrated in Fig. 3, the scoring of these traits is based upon the completeness of fusion, rather than the appearance of any bony bridging.

### *Microporosity*

Microporosity is defined as pits or holes on the cortical auricular surface with a diameter *less than* 1 mm (15). The presence of both microporosity and macroporosity is depicted in Fig. 4.

### *Macroporosity*

Macroporosity is defined as cortical auricular surface pits or holes with a diameter of *more than* 1 mm (15) (see Fig. 4*B*).

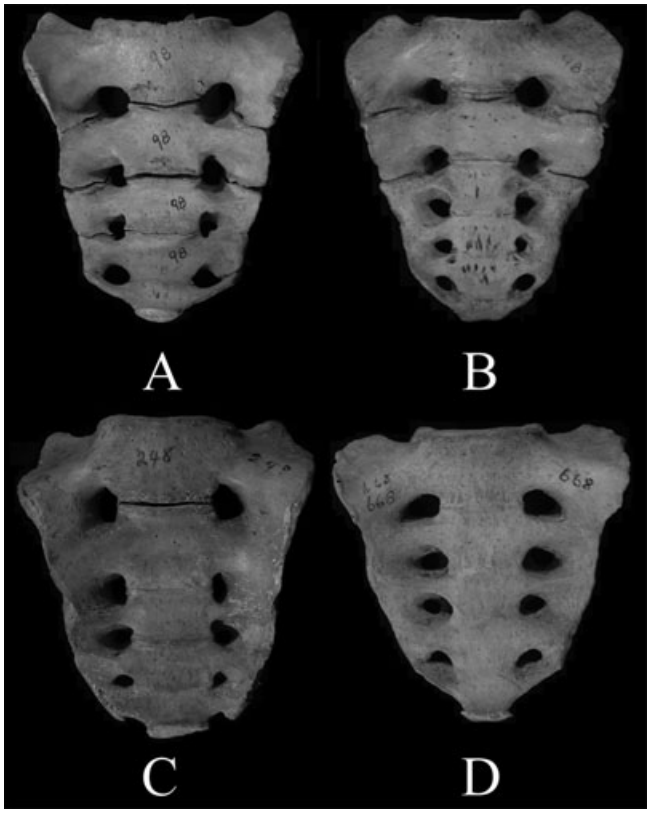


FIG. 3—*Age-related sequencing of sacral body fusion.*

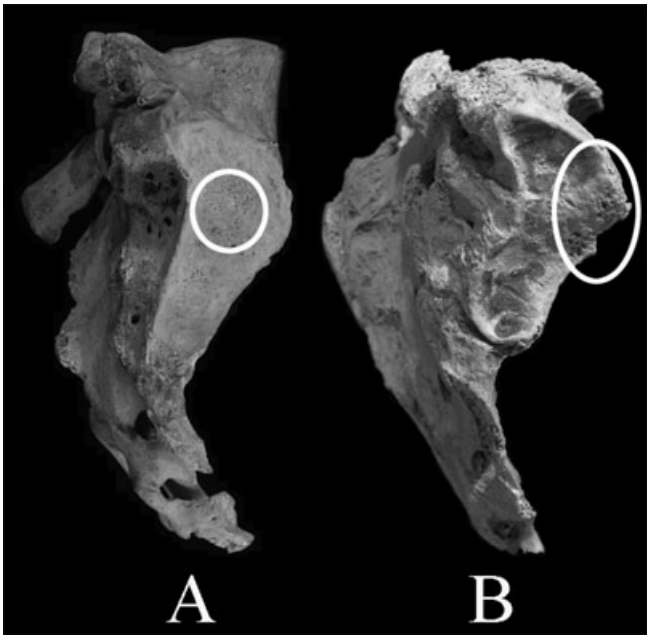


FIG. 4—*Examples of the presence of both micro- (A) and macroporosity (B) occurring on the sacral auricular surface.*

### *Surface Texture*

*Billows* are morphologies similar to those found on the pubic symphyseal surface (7) and the auricular surface of the ilium. They can be manifested as very shallow ridges and furrows but usually are characterized by an uneven surface containing slight depressions and peaks. They appear on the auricular surface early in life

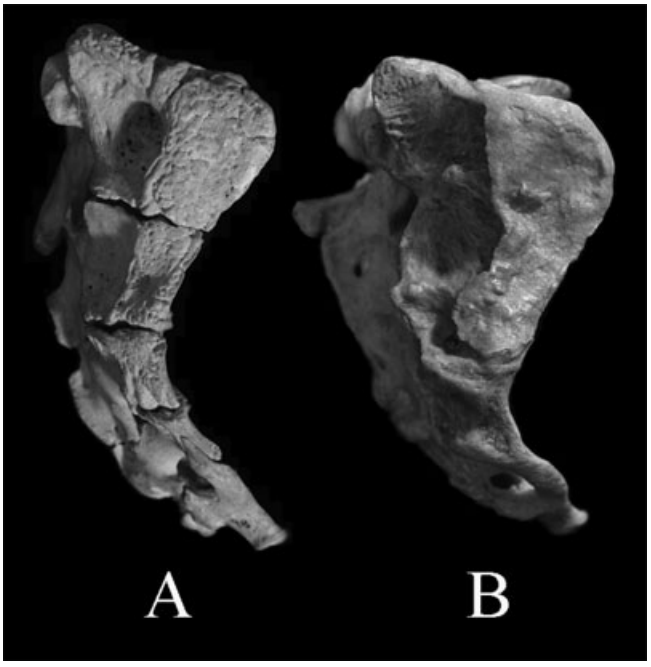


FIG. 5—*Examples of presence (A) and absence (B) of billows on the sacral auricular surface.*

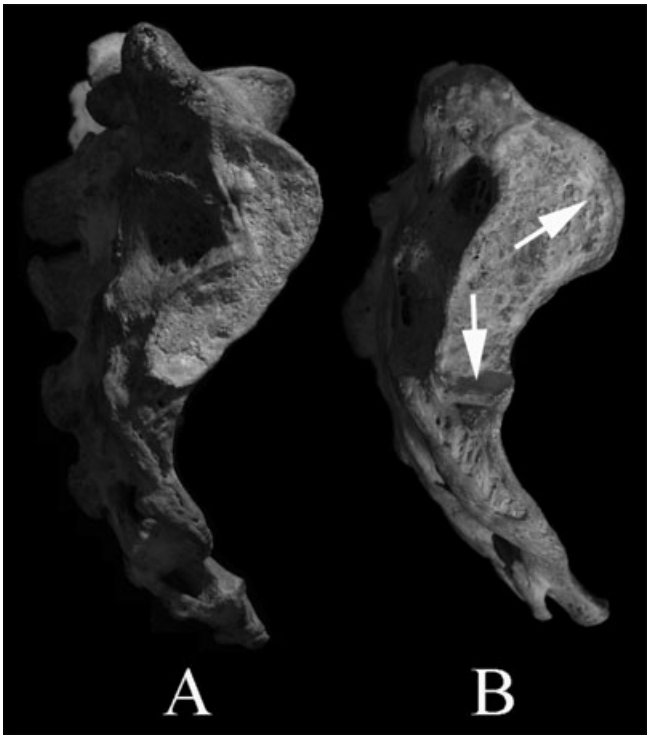


FIG. 6—*Examples of absence (A) and presence (B) of osteoarthritic auricular apical lipping.*

and are observable until a small plate-like epiphysis fuses to the surface which occurs usually in mid to late teens (8).

*Granularity* is a trait usually used in reference to the texture of the auricular surface of the ilium (8,15,16). This trait was omitted in this study due to the ambiguity and complexity of the trait. Billowing is only found in the sacral auricular surface before the fusion of the auricular epiphysis, afterwards the topography is generally smooth or lacking undulations (Fig. 5).

*Osteoarthritic Auricular Apical Lipping (Apical Changes)*

Osteoarthritic auricular apical lipping refers to the osteophytic activity which occurs around the rim of the sacral auricular surface. Lipping is common in older individuals but may not be directly influenced by age (see Discussion). Females tend to show more extreme degrees of apical growth than males, especially at the anterior apex. The presence of auricular apical lipping is defined here as the depression or extension of the narrow rim which appears around the auricular surface (Fig. 6).

*Vertebral Ring Fusion and Absorption (S1 Ring Fusion)*

Vertebral ring fusion and absorption are scored by the degree of fusion or absorption between the superior vertebral epiphysis and the vertebral body (Fig. 7). This is noted for either the first sacral vertebra or a sacralized fifth lumbar vertebra in this study.

*Coccygeal Fusion*

Coccygeal fusion is the fusion of the coccyx to the last sacral vertebral body.

## Results

*General Description of Age-Related Morphological Changes of the Sacrum*

These stages are general descriptions of morphologies with typical, but not statistically validated associated ages and are meant to serve as guides to understanding the aging process in the sacrum, not for generating age-at-death estimates. Furthermore, these "stages" are not equivalents to the following "phases," which are based on the sequential coding component system.

*Stage 1 (<25 years)*—The earliest discrete morphological change noted was the fusion of the third and second sacral vertebrae. At this time, the auricular surface has a billowy appearance with no porosity. The auricular rim does not show any osteophytic activity or lipping and the vertebral ring on the vertebral body of S1 is unfused or fusing.

*Stage 2 (20–30s)*—Individuals in their 20s show fusion of the auricular epiphysis that results in a sacral auricular surface that is relatively smooth (billowing is lost). The second and first sacral vertebrae become fused and the vertebral ring is fusing or completely fused to the body of S1.

*Stage 3 (30–40s)*—Individuals in their 30s typically exhibit some degree of lipping around the auricular surface. In addition, some microporosity and even macroporosity may be present. The condition of the bone is still firm and solid; although it may be becoming lighter, the overall quality is still good.

*Stage 4 (40–50)*—Enhanced levels of microporosity and auricular apical lipping are noted in individuals in the 40s. The overall condition of the bone will begin to deteriorate as the quality of bone becomes lighter.

*Stage 5 (>50)*—The final stage of descriptive morphological changes observed in the sacrum is seen in individuals over the age of 50 years. At this time, the S1 vertebral ring will become absorbed, and macroporosity may be present on the auricular

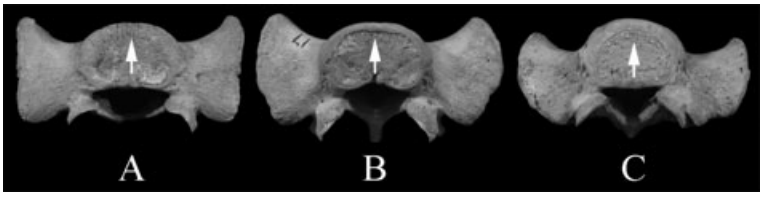


FIG. 7—*Examples of incomplete (A), complete (B), and absorbed (C) sacral vertebral body fusion. Special notice should be paid to the most anterior area, as these changes are often the most pronounced.*

TABLE 1—*Revised trait character states.*

Second and Third Sacral Segment Vertebral Fusion (S2/S3 F)
1 = Incomplete fusion. Refers to any lack of fusion, particularly located on the anterior body or lateral alae (Figs. 2*A* and 2*B*).
2 = Completely fused (Figs. 2*C* and 2*D*).
First and Second Sacral Segment Vertebral Fusion (S1/S2 F)
1 = Incomplete fusion (see above) (Figs. 2*A* and 2*C*).
2 = Completely fused (Fig. 2*D*).
Microporosity (Micro)
1 = No Microporosity is present.
2 = Microporosity is present (Fig. 3*A*).
Macroporosity (Macro)
1 = No Macroporosity is present.
2 = Macroporosity is present (Fig. 3*B*).
Surface Changes
1 = Billowing is present on the sacral auricular surface. Note the lack of fusion between the sacral bodies (Fig. 4*A*).
2 = No billowing is present on the sacral auricular surface. The surface is generally smooth (Fig. 4*B*).
Apical Changes
1 = Apexes are sharp and distinct (Fig. 5*A*).
2 = Lipping and or irregularity is present at the apexes. The auricular surface is slightly depressed to the rim (Fig. 5*B*).
S1 Ring Fusion
1 = Incomplete Fusion. No border on ring. May show a cracked appearance on anterior surface where ring will fuse (Fig. 6*A*).
2 = Fused. Raised border present on anterior aspect of ring with epiphysis completely fused to vertebral body (Fig. 6*B*).
3 = Absorbed. Border no longer raised from surface. The ring has a flattened and/or compressed appearance (Fig. 6*C*).

surface. Additionally, degeneration of many of these features will be observed and the quality of the bone may become very thin and light.

### *Trait Development*

Initial results demonstrated that in most cases, the intermediate trait stages did not contribute significantly to the accuracy or precision of the age estimates, as reflected in even a slightly lower Spearman correlation of trait combination with age when intermediate stages were taken into account ($r = 0.63$; $p < 0.001$) than when the traits were mostly coded as binomial variables (i.e., on a presence–absence basis) ($r = 0.70$; $p < 0.001$). Furthermore, analyses of coccygeal fusion data did not find a significant correlation with age ($\alpha$-level = 0.05). These results significantly simplified the scoring system and served to reduce inter-observer error. Thus, all age estimation was based on the revised character states in Table 1.

TABLE 2—*Sacral trait order in the new coding system.*

| Trait | S2/S3 Fusion | Surface Changes | S1/S2 Fusion | Apical Changes | S1 Fusion | Microporosity | Macroporosity |
|---|---|---|---|---|---|---|---|
| Coding order | 1 | 2 | 3 | 4 | 5 | 6 | 7 |

TABLE 3—*Original and revised phases, unique codes, and description of traits present.*

| Original Phase | Revised Phase | Code | Trait Appearance |
|---|---|---|---|
| 1 | 1 | 1111111 | No porosity, lipping, or complete fusions |
| 2 | 2 | 2211211 | S2/S3 fusion complete, auricular plate fused, S1 ring fused |
| 3 | 3 | 2221211 | S1/S2 fusion complete |
| 4 | 4 | 2222211 | Lipping present on apex |
| 5 | 4 | 2222221 | Microporosity present, S1 ring unabsorbed |
| 6 | 5 | 2222311 | S1 ring absorbed, no porosity present |
| 7 | 6 | 2222321 | S1 ring absorbed with microporosity present |
| 8 | 6 | 2222322 | S1 ring absorbed with macroporosity present |

### *Component System Development*

The results of the initial phase of study suggested that by including both developmental and degenerative features in the analysis, the seven traits described above could be sequentially arranged to reflect the differential timing of significant aging events. This indicated that clearly defined morphological changes could be used to create a significant age sequence. The order of appearance of each trait within the seven-digit code was calculated to maximize the Spearman's rank correlation coefficient of the code with age (Table 2).

### *Methodological Analyses*

Based on the similarities in mean age and the overlap in confidence intervals for both phases 4 and 5 as well as phases 7 and 8, *t*-tests were performed to assess the inter-group mean differences. Results indicate that, even before Bonferroni correction, the mean ages of these phases are not significantly different. Thus, phases 4 and 5 and phases 7 and 8 were collapsed into phase 4 and phase 6 respectively, creating a system of six revised phases. Table 3 presents the original and revised phases with their associated code scores and trait descriptions to illustrate the coding process and how the code is affected by changes in trait scores.

To test for significant differences between left and right sides of the sacrum, a *t*-test was conducted. Results showed no significant differences between left and right scoring. Consequently, whenever there was a discrepancy between sides, the older side was favored (28).

### *Sample Testing*

The coding system was developed independently on both European American males ($n = 152$) and females ($n = 90$) from the Hamann-Todd Collection and then tested on independent Bass collection samples. For European American males, the method proved accurate (93.3% correct) for all phases when tested on the Bass sample ($n = 160$). These samples then were pooled into one

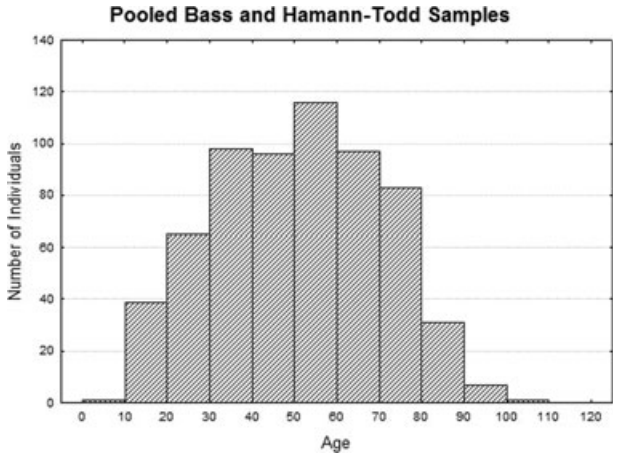


FIG. 8—*Final age distribution of pooled subsamples.*

TABLE 4—*Age estimates by phase.*

| Phase | Mean Age | 68% Range | 95% Range | *n* | S | Median Age | Min Age | Max Age | Inaccuracy |
|---|---|---|---|---|---|---|---|---|---|
| 1 | 16.11 | 13–16 | 9–23 | 19 | 3.38 | 17 | 10 | 24 | 2.63 |
| 2 | 23.05 | 20–26 | 17–29 | 22 | 3.05 | 23 | 19 | 29 | 2.6 |
| 3 | 27.96 | 19–37 | 10–46 | 56 | 9.23 | 26.5 | 16 | 71 | 6.6 |
| 4 | 45.39 | 31–45 | 16–75 | 142 | 14.89 | 43.5 | 18 | 93 | 12.09 |
| 5 | 50.82 | 36–67 | 21–81 | 66 | 15.09 | 47.5 | 24 | 96 | 12.39 |
| 6 | 62.79 | 49–77 | 35–91 | 328 | 14.04 | 63 | 30 | 97 | 11.57 |

European American male sample. The same analyses were conducted using the European American females from the Hamann-Todd ($n$ = 89) and Bass collections ($n$ = 89). This too proved accurate (98.5% correct). The samples then were pooled into one European American female cohort. The new European American male method then was applied to the European American female sample to test for sex differences. Again, the method was accurate (96.7% correct) and the samples were pooled into one European American sample. Finally, the European American sample was tested on the African American male ($n$ = 76) and female ($n$ = 68) samples from the Haman-Todd collection, the method proved 96.3% correct and 99.1% correct, respectively. All the groups were then pooled, creating one final method ($n$ = 634, Fig. 8) consisting of a six-phase system. All phase data and associated descriptive statistics are presented in Table 4.

## Discussion

The sacrum can be used for both developmental and degenerative age-at-death predictions. The descriptive stages of age progression presented here are to be used as guides in understanding general morphological changes over time and not as categorical phases for age-at-death estimation. Only the phase method based on binomial character states has statistically determined confidence intervals and is suitable for unknown age assessment. Based on the character states of the presented traits as well as their usage in the sequential coding component system, several points of discussion are relevant.

The presented traits are not independent, and tend to appear in regular combinations. Using the coding method, eight different phases were observed more often than apparently random or epipathological combinations or traits. *T*-tests confirmed that there were no significant differences between two sets of phases, thus reducing the eight-phase system to a six-phase system. The result is a robust indicator of forensic age-at-death which appears to have no sex or ancestry specific biases.

Auricular surface apical lipping, vertebral ring absorption, microporosity, and macroporosity are all secondary degenerative aging functions and therefore act differently from developmental processes (25). The process of degenerative aging actually is a slow accumulation of bony changes which occur as a function of environmental and genetic interactions on a much more complex level than those of development. This is directly reflected in the wider age ranges after development has ceased (here, phases 4–6). During development, the changes with age are much more regulated by genetic processes; for instance, the fusion of the sacral bodies occurs in a very consistent and reliable pattern with S2/S3 fusion occurring before S1/S2 fusion in over 99% of the final pooled sample. Furthermore, the breakdown of sacral body fusion by age class is fairly consistent with the original results obtained by McKern and Stewart (5).

While auricular surface microporosity tends to occur at younger ages than macroporosity, when considering variation in timing for both macro- and microporosity final age ranges are nearly identical. This therefore requires the collapsing of the last two phases into one (phase 6). The etiology of auricular porosity is not well understood but it may result from subperiosteal irritation or stress or microtrauma due to mechanical stresses. Similarly, lipping to the apexes of the auricular surface and absorption of the first sacral vertebral disk are likely arthritic in origin and probably linked to activity patterns, as well as physical stressors. Again, while correlated with age they are degenerative aging features, not direct features of aging; thus these criteria produce wider age ranges than developmental traits. These features can be used to determine adult chronological age in a general sense, but remain inaccurate and imprecise. While this may be a function of the character states being too robust to detect more fine morphological changes, the current attempt at quantifying degenerative features found the presence–absence scales to be more applicable. Finally, the "older" sacral auricular surface should always be favored in analyses when discrepancies occur. The more advanced configuration should be more accurate because to express an older set of traits, this region must have passed through the "younger" morphologies (phases) making the older side the more accurate indicator of age at death (as demonstrated in 28).

## Conclusions

It was found in this study that scoring traits on a presence–absence basis rather than the assessment of multiple character states significantly increased the correlation to chronological assessments to age. This may be best explained by the reduction in inconsistency of trait scoring resulting in a significant reduction in inter- and intraobserver error. It may also be related to a greater amount of variability in the duration of certain trait stages.

The results of this study clearly indicate that the sacrum can be used for generating forensically significant age-at-death estimates. This method utilizes seven developmental and degenerative traits which are assessed through presence–absence scoring. By presenting both one and two standard deviation ranges of error, the method has utility in both bioarchaeological and forensic anthropological settings.

This method is similar to other forensic-based age estimation methods in that it is best suited for inclusion with multiple age marker methods and not as a stand-alone technique. This is vital to forensic age estimation and is a common theme for most

forensically applied methods. While the confidence intervals of all methods must be set at two standard deviations (95% probabilities), these ranges are far too wide to be of much use in providing a possible match from a missing persons list. All of the age estimation methods based on skeletal attributes available should be used in conjunction with one another in order to provide the most precise estimation of age possible.

*Acknowledgments*

The author would like to thank the collection managers, specifically Mr. Lyman Jellema of the Cleveland Museum of Natural History and Dr. Lee Meadows Jantz of the University of Tennessee, Knoxville. Additional thanks to Dr. Dennis Dirkmaat, Dr. Steven Symes, Mr. Luis Cabo, and Mr. Christopher Rainwater for their contributions to this research.

## References

1. Weiss KM. Demographic models for anthropology. District of Columbia: The Society for American Archaeology, 1973.
2. Hoppa RD, Vaupel JW, editors. Paleodemography: age distributions from skeletal samples. Cambridge: Cambridge University Press, 2002.
3. Meindl RS, Lovejoy CO. Ectocranial suture closure: a revised method for the determination of skeletal age at death based on the lateral-anterior suture. Am J Phys Anthropol 1985;68:57–66.
4. Nawrocki SP. Regression formulae for estimating age at death from cranial suture closure. In: Reichs KJ, editor. Forensic osteology: advances in the identification of human remains. Springfield: Thomas, 1998;276–92.
5. McKern TW, Stewart TD. Skeletal age changes in young American males. Natick, MA: Environmental Protection Research Division, Quartermaster Research and Development Center, 1957 Technical Report: EP-45.
6. Scheuer L, Black S. Developmental juvenile osteology. San Diego, CA: Academic Press, 2000.
7. Suchey JM, Katz D. Applications of pubic age determination in a forensic setting. In: Reichs KJ, editor. Forensic osteology: advances in the identification of human remains. Springfield: Thomas, 1998;204–36.
8. Lovejoy CO, Meindl RS, Pryzbeck TR, Mensforth RP. Chronological metamorphosis of the auricular surface of the ilium: a new method for determination of adult skeletal age at death. Am J Phys Anthropol 1985;68(1):15–28.
9. Osborne DL, Simmons TL, Nawrocki S. Reconsidering the auricular surface as an indicator of age at death. J Forensic Sci 2004;49(5):905–11.
10. İşcan MY, Loth SR, Wright RK. Age estimation from the rib by phase analysis: white females. J Forensic Sci 1985;30:853–63.
11. Prince DA, Ubelaker DH. Application of Lamendin's adult dental aging technique to a diverse skeletal sample. J Forensic Sci 2002;47(1):107–16.
12. Ousley S. Should we estimate biological or forensic stature? J Forensic Sci 1995;40(5):768–73.
13. United States Supreme Court in Daubert v. Merrell Dow Pharmaceuticals, Inc., 509 U.S. 579, 1993.
14. Ritz-Timme R, Cattaneo C, Collins MJ, Waite ER, Shultz HW, Kaatsch HJ, et al. Age estimation: the state of the art in relation to the specific demands of forensic practice. Int J Legal Med 2000;113:129–36.
15. Buckberry JL, Chamberlain AT. Age estimation from the auricular surface of the ilium: a revised method. Am J Phys Anthropol 2002;119:231–39.
16. Igarashi Y, Uesu K, Wakebe T, Kanazawa E. New method for estimation of adult skeletal age at death from the morphology of the auricular surface of the ilium. Am J Phys Anthropol 2005;128(2):324–39.
17. Falys G, Schutkowski H, Weston DA. Auricular surface aging: worse than expected? A test of the revised method on a documented historic skeletal assemblage. Am J Phys Anthropol 2006;130(4):508–13.
18. Sashin D. A critical analysis of the anatomy and pathologic changes of the sacro-iliac joints. J Bone Joint Surg Am 1930;12:891–910.
19. Bollow M, Braun J, Kannenberg J, Biedermann T, Schauer-Petrowskaja C, Paris S, et al. Normal morphology of sacroiliac joints in children: magnetic resonance studies related to age and sex. Skeletal Radiol 1997;26:697–704.
20. Shibata Y, Shirai Y, Miyamoto M. The aging process in the sacroiliac joint: helical computed tomography analysis. J Orthop Sci 2002;7:12–18.
21. Albert AM, Maples WR. Stages of epiphyseal union for thoracic and lumbar vertebral centra as a method of age determination for teenage and young adult skeletons. J Forensic Sci 1995;40(4):623–33.
22. Albert AM. The use of vertebral ring epiphyseal union for age estimation in two cases of unknown identity. Forensic Sci Int 1998;97:11–20.
23. Drukier P, Sarajlic N, Klonowski E. Age related changes in the adult male vertebral column. Proceedings of the 55th Annual Meeting of the American Academy of Forensic Sciences, 2003 February 17–22, Chicago, IL. Colorado Springs, CO: American Academy of Forensic Sciences, 2003;249–50.
24. Klonowski E, Sarajlic N, Drukier P, Klonowski AM. The impact of age related changes in the vertebral column on age determination for identification purposes. Proceedings of the 57th Annual Meeting of the American Academy of Forensic Sciences, 2005 February 21–26, New Orleans, LA. Colorado Springs, CO: American Academy of Forensic Sciences, 2005;326–27.
25. Lovejoy CO, Meindl RS, Mensforth RP, Barton TJ. Multifactorial determination of skeletal age at death: a method and blind tests of its accuracy. Am J Phys Anthropol 1985;68(1):1–14.
26. Masset C. Age estimation on the basis of cranial sutures. In: Iscan MY, editor. Age markers in the human skeleton. Springfield: Thomas, 1989;71–104.
27. Zambrano CJ. Evaluation of regression equations used to estimate age at death from cranial suture closure [thesis]. Indianapolis, IN: University of Indianapolis, 2005.
28. Overbury RS. Asymmetry of the pubic symphyseal face and femora [thesis]. Erie, PA: Mercyhurst College, 2007.

Additional information and reprint requests:
Nicholas V. Passalacqua, M.S.
Department of Anthropology
Michigan State University
354 Baker Hall
East Lansing, MI 48824
E-mail: passala5@msu.edu